Controlled Permeability in Polyelectrolyte Films via Solvent Treatment

Wen-Fei Dong,*,† Shaoqin Liu,†,# Lei Wan,‡ Guangzhao Mao,‡ Dirk G. Kurth,†,§ and Helmuth Möhwald†

Max Planck Institute of Colloids and Interfaces, Golm/Potsdam, D-14476, Germany, Department of Chemical Engineering and Materials Science, Wayne State University, 5050 Anthony Wayne Drive, Detroit, Michigan 48202, and National Institute for Materials Science (NIMS), 1-1 Namiki, Tsukuba, Ibaraki 305-0044, Japan

Received May 21, 2005. Revised Manuscript Received August 3, 2005

The influence of solvents (alcohols and binary mixtures of alcohol and water) on the structure and permeability of self-assembled layer-by-layer polyelectrolyte multilayers (PEMs) has been investigated by in situ atomic force microscopy (AFM), cyclic voltammetry (CV), and confocal laser scanning microscopy (CLSM). A decrease in the dielectric constant of the solvent medium increases the strength of electrostatic interactions between the polyelectrolyte chains because the Coulombic force is inversely proportional to the dielectric constant. The stronger attractions as a result of increased alcohol volume percentage in water drive the polyelectrolyte chains to contract, collapse, and coagulate. Consequently, subtle changes in the PEM film structure are observed. AFM images show that the originally smooth surface of the PEM film becomes rougher with aggregates and holes developing with increasing alcohol amount. The diffusion of $Fe(CN)_6^{3-/4-}$ through PEM films is promoted upon solvent treatment. The entrapment of $Fe(CN)_6^{3-/4-}$ in the film occurs at a high amount of ethanol content (>60%). The permeability of large macromolecules, i.e., dextran with molecular weight of 66 kDa, to polymeric capsules is also enhanced by solvent treatment. By the methods of "additional PEM coating" and solvent treatment, the mesh size of capsules becomes tunable as does the capsule permeability. The conversion between microporous capsules to mesoporous capsules has a potential application in smart encapsulation and controlled delivery.

Introduction

Polymeric ultrathin films find numerous applications in the fields of surface engineering, such as printing, coating, tissue engineering, and biosensing.[1−8] Continuous efforts are being made to seek simple, cheap, and time-effective preparation methods for thin films. Recently, a novel type of stratified polyelectrolyte thin films (PEMs) has been created via the alternating deposition of oppositely charged polyelectrolytes onto substrates.[6−8] The interests of these films stem from their tunable functionality, well-defined structure, accurate thickness control, and versatile and aqueous-based preparation procedures on substrates of any shapes. Increasing attention has been directed to the potential application of these PEMs in the fields of drug delivery and gene therapy. A prerequisite for this is the understanding and manipulation of the PEM films.

External stimuli had been utilized to control the mass transport and morphology within PEMs, for instance, ionic strength,[9,10] pH,[11−14] temperature,[15−17] post chemical reaction,[18−23]metal ion coordination,[24] and electric field.[25,26]

---

[*] To whom correspondence should be addressed. E-mail: dong@mpikg-golm.mpg.de. Tel: +49 331 567 9257. Fax: +49 331 567 9202.

[†] Max Planck Institute of Colloids and Interfaces.

[‡] Wayne State University.

[§] NIMS.

[#] Permanent address: Changchun Institute of Applied Chemistry, Chinese Academy of Sciences, Changchun 130022, People's Republic of China.

(1) Erbil, H. Y.; Demirel, A. L.; Avci, Y.; Mert, O. *Science* **2003**, *299*, 1377.
(2) Stamm, M.; Minko, S.; Tokarev, I.; Fahmi, A.; Usov, D. *Macromol. Symp.* **2004**, *214*, 73.
(3) Decher, G.; Hong, J. D.; Schmitt, J. *Thin Solid Films* **1992**, *210*, 831.
(4) Krasemann, L.; Toutianoush, A.; Tieke, B. *J. Membr. Sci.* **2001**, *181*, 221.
(5) Tieke, B.; Krasemann, L.; Toutianoush, A. *Macromol. Symp.* **2001**, *163*, 97.
(6) Donath, E.; Sukhorukov, G. B.; Caruso, F.; Davis, S. A.; Mohwald, H. *Angew. Chem., Int. Ed.* **1998**, *37*, 2202.
(7) Sukhorukov, G. B.; Donath, E.; Davis, S.; Lichtenfeld, H.; Caruso, F.; Popov, V. I.; Mohwald, H. *Polym. Adv. Technol.* **1998**, *9*, 759.
(8) Dong, W. F.; Sukhorukov, G. B.; Mohwald, H. *Phys. Chem. Chem. Phys.* **2003**, *5*, 3003.
(9) McAloney, R. A.; Sinyor, M.; Dudnik, V.; Goh, M. C. *Langmuir* **2001**, *17*, 6655.
(10) Voegel, J. C.; Decher, G.; Schaaf, P. *Actualite Chim.* **2003**, 30.
(11) Hiller, J.; Mendelsohn, J. D.; Rubner, M. F. *Nat. Mater.* **2002**, *1*, 59.
(12) Sui, Z. J.; Schlenoff, J. B. *Langmuir* **2004**, *20*, 6026.
(13) Lulevich, V. V.; Vinogradova, O. I. *Langmuir* **2004**, *20*, 2874.
(14) Sukhorukov, G. B.; Antipov, A. A.; Voigt, A.; Donath, E.; Mohwald, H. *Macromol. Rapid Commun.* **2001**, *22*, 44.
(15) Tan, H. L.; McMurdo, M. J.; Pan, G. Q.; Van Patten, P. G. *Langmuir* **2003**, *19*, 9311.
(16) Gao, C. Y.; Leporatti, S.; Moya, S.; Donath, E.; Mohwald, H. *Chem.-Eur. J.* **2003**, *9*, 915.
(17) Dautzenberg, H.; Gao, Y. B.; Hahn, M. *Langmuir* **2000**, *16*, 9070.
(18) Vuillaume, P. Y.; Jonas, A. M.; Laschewsky, A. *Macromolecules* **2002**, *35*, 5004.
(19) Welsh, E. R.; Schauer, C. L.; Santos, J. P.; Price, R. R. *Langmuir* **2004**, *20*, 1807.
(20) Richert, L.; Engler, A. J.; Discher, D. E.; Picart, C. *Biomacromolecules* **2004**, *5*, 1908.
(21) Dai, J. H.; Jensen, A. W.; Mohanty, D. K.; Erndt, J.; Bruening, M. L. *Langmuir* **2001**, *17*, 931.
(22) Harris, J. J.; Bruening, M. L. *Langmuir* **2000**, *16*, 2006.
(23) Harris, J. J.; Stair, J. L.; Bruening, M. L. *Chem. Mater.* **2000**, *12*, 1941.
(24) Krass, H.; Papastavrou, G.; Kurth, D. G. *Chem. Mater.* **2003**, *15*, 196.

10.1021/cm051090f CCC: $30.25

Recently, organic solvent treatment has been investigated in order to demonstrate its effects on the structure, mechanic properties, and permeability of the thin films.[8,27−30] For instance, the PEM film thickness increases when a binary solvent mixture of ethanol and water is used during the multilayer assembly;[27,29] the mechanical properties of PEM-based hollow capsules have been found to decrease significantly after solvent treatment.[28,31] Solvent treatment has also played an important role on the encapsulation[28,30] and optical properties of hollow PEM capsules.[8] These findings demand further understanding of the molecular mechanisms underlying the solvent effect. Solvent-induced swelling of polylysine and polyacrylate multilayers has been investigated by ATR-FTIR spectroscopy.[32] It provides evidence of an increase in the polymer segment density due to the addition of ethanol in water. The effect of solvent on the polymer conformation is applied by the solvent−polymer interaction. Therefore, by controlling their inner chemical structures, PEM membranes have been used to separate water and alcohol mixtures.[33] On the other hand, in the case of lipid-coupled PEM systems, the addition of ethanol to the aqueous solution has been shown to induce the faster diffusion of lipid molecules on the PEM films, which is attributed to the diffusion of the solvent molecule into the polyelectrolyte−lipid interface and then coupling strength is weakened.[34] However, the microstructure of the PEM substrate responsive to such local environmental changes has not been fully addressed.

In our recent paper,[35] stable and robust capsules had been produced by the polyelectrolyte pair of poly(styrene sulfonate) (PSS) and poly(allylamine hydrocloride) (PAH) on weakly cross-linked melamine formaldehyde (MF) particles as sacrificial cores. With control of the PEM film thickness and core removal conditions, two different intact capsules are obtained in term of mesh size, which are so-called microporous and mesoporous capsules, respectively. Mesoporous capsules have a big mesh size to allow large macromolecular passing easily, but microporous capsules do not. Several groups reported the results about the solvent effects on permeability and mechanic properties of microporous capsules.[28,30] However, to our knowledge, the studies of solvent treatment on permeability of mesoporous capsules are rare.

In this paper, two main goals are pursued: one is to control the permeability of mesoporous capsules by solvent treatment and the other is to explain the phenomena of the microstructure changes in PEM films after solvent treatment. A simple and easy method of "PEM coating + solvent treatment" is used to control capsule permeability by switching the mesh size of the capsule wall, as shown in Figure 1. Here, mesoporous MF capsules are used as a soft organic template.[35] As known, additional PEM coating can produce a dense, porous-free, and small mesh-sized thin film on these porous capsules.[35] These films limit the penetration of large macromolecules to capsules.[36] However, the macromolecules become permeable to capsules after solvent treatment. Thus, several circles of "PEM coating + solvent treatment" can be utilized to switch the permeability of capsules. To understand the mechanism of the solvent effect, in situ measurements have to be carried out in the solution. The experimental results are divided into three parts. In part one, confocal laser scanning microscopy (CLSM) is used to investigate the solvent effect on mesh-sized PEM-coated capsules. After immersion in the alcoholic solvent for an extended time (>12 h), the capsule mesh size increases to several times that of the original capsule prior to the solvent treatment. In part two, electrochemical measurements shed light on the PEM film permeability and structural changes during solvent diffusion.[21,22,37−39] Part three shows in situ AFM results of the PEM surface morphological changes in different solvent conditions. Finally, the mechanism of solvent effect is discussed.

Experimental Section

Materials. Poly(styrene sulfonate) sodium salt (PSS, Mw ~ 70 kDa), poly(allylamine hydrochloride) (PAH, Mw ~ 70 kDa), polyethylenimine (PEI, Mw ~ 25 kDa), rhodamine isothiocyanate labeled dextran (TRITC-dextran Mw ~ 4 kDa or Mw ~ 66 kDa), $K_3Fe(CN)_6$, 3-aminopropyltrimethoxysilane, methanol, ethanol, 2-butanol, potassium chloride, and sodium chloride are purchased from Aldrich. Weakly cross-linked melamine formaldehyde particles (MF particles, diameter $= 5.0 \pm 0.2\ \mu$m) are obtained from Microparticles GmbH, Germany. All chemicals are used as received except for PSS, which is dialyzed before use to remove molecules with molecular weight lower than 50 kDa. Water used in all experiments is purified in a three-stage Milli-Q Plus 185 purification system and has an initial resistivity higher than 18.2 MΩ·cm.

Multilayer Preparation. PEMs are built up by the dipping-assembly method on mica or ITO substrate. For example, the cleaned ITO-coated glass electrode is first functionalized with 3-aminopropyltrimethoxysilane to yield an amine-functionalized thin film by immersing the ITO electrode into a 10^{-2} mol/L toluene solution overnight.[40] The ITO electrode is then immersed in the PSS solution (1 mM; with or without 0.5 mM NaCl) for 10 min and rinsed with water. The PSS-coated electrode is then immersed in PAH (1 mM; with or without 0.5 mM NaCl) for 10 min to deposit the polycation/polyanion bilayer film. The above procedure is repeated to deposit additional bilayers. Between each deposition, the dipping-assembled PEM film is dried. In the case of mica, a layer of PEI is first deposited by immersing mica in 10 mM PEI

---

(25) Kurth, D. G.; Lopez, J. P.; Dong, W. F. *Chem. Commun.* **2005**, 2119.
(26) Sun, J.; Gao, M.; Feldmann, J. *J. Nanosci. Nanotechnol.* **2001**, *1*, 133.
(27) Poptoshev, E.; Schoeler, B.; Caruso, F. *Langmuir* **2004**, *20*, 829.
(28) Kim, B. S.; Lebedeva, O. V.; Koynov, K.; Gong, H.; Glasser, G.; Lieberwith, I.; Vinogradova, O. I. *Macromolecules* **2005**, *38*, 5214. Article.
(29) Dubas, S. T.; Schlenoff, J. B. *Macromolecules* **1999**, *32*, 8153.
(30) Lvov, Y.; Antipov, A. A.; Mamedov, A.; Mohwald, H.; Sukhorukov, G. B. *Nano Lett.* **2001**, *1*, 125.
(31) Vinogradova, O. I. *J. Phys.-Condens. Matter* **2004**, *16*, R1105.
(32) Muller, M.; Heinen, S.; Oertel, U.; Lunkwitz, K. *Macromol. Symp.* **2001**, *164*, 197.
(33) Toutianoush, A.; Krasemann, L.; Tieke, B. *Colloids Surf. A* **2002**, *198*, 881.
(34) Wang, L. Y.; Schonhoff, M.; Mohwald, H. *J. Phys. Chem. B* **2004**, *108*, 4767.
(35) Dong, W. F.; Ferri, J. K.; Adalsteinsson, T.; Schonhoff, M.; Sukhorukov, G. B.; Mohwald, H. *Chem. Mater.* **2005**, *17*, 2603.
(36) Ibarz, G.; Dahne, L.; Donath, E.; Mohwald, H. *Macromol. Rapid Commun.* **2002**, *23*, 474.
(37) Saveant, J. M. *J. Electroanal. Chem.* **1991**, *302*, 91.
(38) Farhat, T. R.; Schlenoff, J. B. *Langmuir* **2001**, *17*, 1184.
(39) Pardo-Yissar, V.; Katz, E.; Lioubashevski, O.; Willner, I. *Langmuir* **2001**, *17*, 1110.
(40) Kurth, D. G.; Bein, T. *Langmuir* **1995**, *11*, 3061.

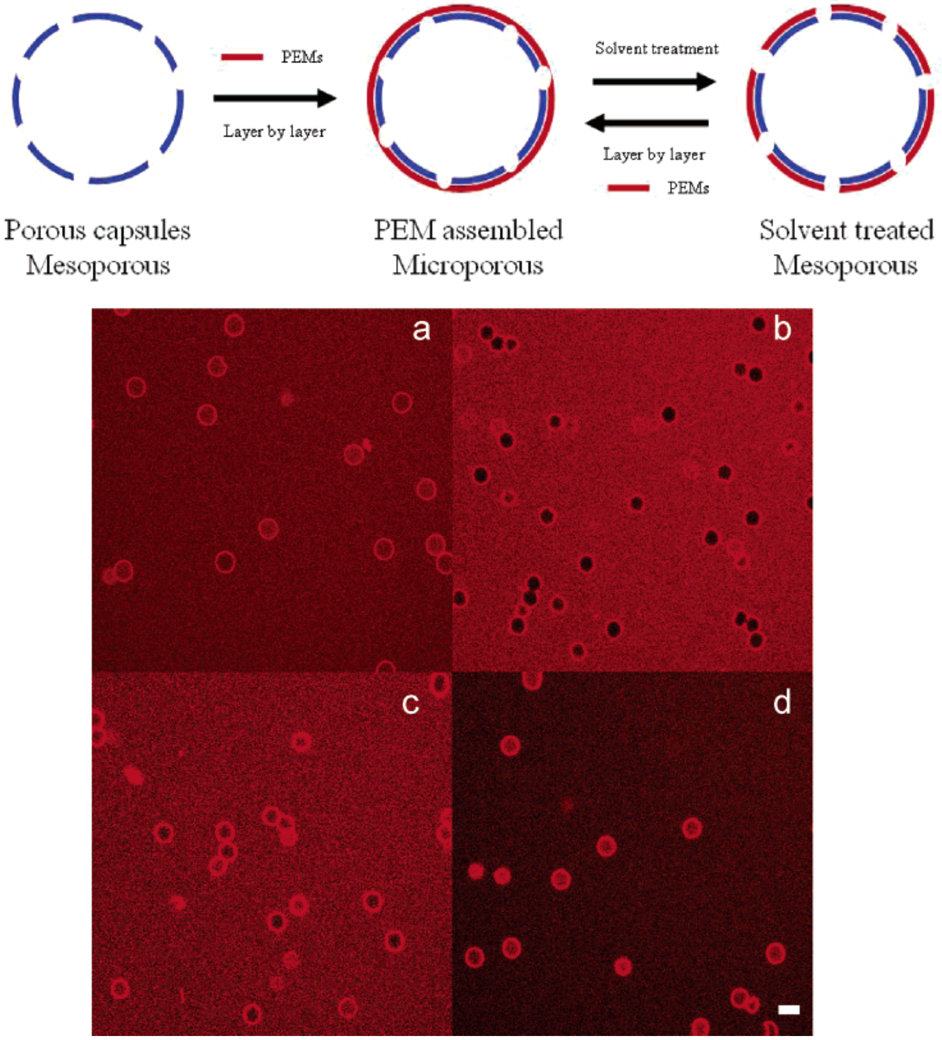

Figure 1. CLSM imaging of (a) mesoporous capsule $(PSS/PAH)_5$, (b) capsule (a) modified by additional layers of PSS/PAH, (c) capsule (b) after 1 h treatment with 50% ethanol solution, and (d) capsule (b) after 12 h solvent treatment. The probe material is the TRITC-dextran with 66 kDa. Scale bar is 5 μm. The graphic above the figure shows the method of "PEM coating + solvent treatment" to control the permeability of capsules (from microporous to mesoporous by switching the mesh sizes of capsules). The details are reported in the text.

solution for 10 min followed by rinsing and drying. The subsequent PSS/PAH assembly is the same as that on the ITO electrode.

Porous PEM Capsule Preparation. Hollow PEM microcapsules are made by stepwise adsorption of polyelectrolyte layers onto a charged colloidal MF template with the colloidal template dissolved and removed in the end.[6−8] A typical recipe for capsule formation is as follows. One milliliter of aqueous PSS solution (5 mg/mL, with 0.5 or 1.0 M NaCl) is added to 1.0 mL of the positively charged MF particle dispersion. The particle concentration is approximately 10^8 particles/mL. The dispersion is stirred during the adsorption time of 20 min at 283 K. Low temperatures are used to minimize the post-polymerization of MF particles, which can lead to increased stability of the core against acid dissolution. The dispersion is centrifuged at 1000*g* for 5 min at 283 K. The supernatant is decanted. The particle precipitants is redispersed by adding 2.0 mL of water with gentle shaking. The centrifugation/washing/redispersion cycle is repeated an additional 3 to 4 times to ensure complete removal of free polyelectrolyte from the dispersion. Subsequent PAH (1.0 mL, 2 mg/mL, 0.5 M NaCl) and PSS layers are deposited onto the colloidal template using the same procedures. PSS and PAH concentrations are well above the concentration necessary for full coverage of the particles. In the last step the MF particle core is dissolved using dilute HCl (pH = 1.0) solution for 20 min. The dissolved species and HCl are removed by centrifuging the dispersion at 3000*g* for 10 min at room temperature. The remaining capsules are washed using the centrifugation/washing/redispersion cycle as described above until neutral pH is established.

PEM-Modified Capsule Preparation. The capsules made by dissolving MF cores tend to have porous shells. To reduce and tune the mesh size, additional PEMs are assembled on the porous capsules.[36] The additional PEMs are assembled similarly as described above. Here, 1 mg/mL PSS and 1 mg/mL PAH are used. Then 1 mL of capsule dispersion is mixed with 1 mL of PSS solution. After incubation for 20 min, the supernatant is removed and the remaining capsules are rinsed by redispersing them in water three times. Subsequent layers are assembled by the same way.

Electrochemical Measurements. Electrochemical measurements are performed in a single-compartment cell with a standard three-electrode configuration: Ag/AgCl/KCl (concentration = 3 mol/L) as the reference electrode, a platinum gauze of large surface area as the counter electrode, and the bare or PEM-coated ITO glass slide as the working electrode. A 0.05 M KCl aqueous or water/alcohol solution of 5 mM $K_3Fe(CN)_6$ is used for the electrochemical measurements. All measurements are carried out at room temperature (~293 K).

Confocal Laser Scanning Microscopy. The permeability of individual capsules is determined by an inverse confocal laser scanning microscope (CLSM, Leica TCS NT, Germany) with either a 100× or a 40× oil immersion objective (numerical aperture = 1.0). Prior to permeability measurements, the capsule solution is mixed with a probe material solution (TRITC-labeled dextran with 66 kDa) for 12 h. Florescence images are recorded within 1 s at the excitation wavelength of 552 nm.

Atomic Force Microscopy (AFM). Multimode IIIa AFM from Digital Instruments with an E-scanner (maximum scan area = 16 × 16 μm^2) is used. Standard silicon nitride probes with a manufacturer-specified spring constant of 0.06 N/m are used in liquid-contact and liquid-tapping experiments. Prior to in situ AFM experiments, PEI/(PSS/PAH)$_2$ with PEI as the bottom layer and PAH as the top layer is assembled on mica by the dipping assembly. The PEM-covered mica piece is fixed on an AFM sample disk and placed in the liquid cell (Digital Instruments). The surface is first imaged in air before injecting the solvent. After the tip and substrate surface are placed in close proximity, the solvent (water, ethanol, ethanol/water mixture, or 2-butanol) is introduced through an inlet tubing and is sealed by an O-ring. Scanning can start within 5 min of solvent introduction. The results reported here are obtained between 10 min and several hours after solvent introduction. The structures are considered in equilibrium because no changes are observed during the period of observation. In liquid-contact mode, height, deflection, and friction images (only height images at high gains are shown here) are captured simultaneously, each containing 256 × 256 pixels. The PEM film can be easily damaged by the scanning motion, and therefore the force need for imaging is always minimized and previously scanned areas are re-scanned at a larger scan area. Images are displayed and analyzed using Nanoscope software from Digital Instruments (Version 5.12). Height images are plane-fit in the fast scan direction with no additional filtering operations. The root-mean-square surface roughness (R_q) is calculated from variations in AFM height images taken from the mean data plane according to

$$R_{\mathrm{q}} = \sqrt{\frac{\sum z_i^{\,2}}{n}}$$

where z_i is the height value and n is the number of pixels in an image. Only R_q numbers of the same scan size (0.5 × 0.5 μm^2) are compared.

Results and Discussion

The air-dried PEM films of (PSS/PAH)$_{10}$ do not lose any materials after 24 h or longer immersion in a number of organic solvents including polar solvents such as methanol, ethanol, and 2-butanol and nonpolar solvents such as chloroform, toluene, and hexane, inconsistent with previous reports.[8,28,31,34] Organic solvents, although do not cause polyelectrolyte to desorb,[27,29,32] tend to reorganize the polyelectrolyte complexes within the assembly as evidenced by the permeability and morphological changes.

Solvent-Switched Mesh Size of Capsules. The diffusion of large macromolecules (i.e., dextran) through capsules is measured by CLSM. In this experiment, TRITC labeled dextran is used as a typical probe because it maintains a stable spherical shape in water and its hydrodynamic radius is controlled by the molecular weight, i.e., TRITC-dextran of 66 kDa has a hydrodynamic radius of 9.0 nm while the radius of 4 kDa TRITC-dextran is about 2.1 nm.[35] On the other hand, TRITC emits fluorescence and shows a red color in the CLSM images when excited by a 552-nm laser. Prior to the measurement, TRITC-dextran is added to the capsule solution. After 24 h, a droplet of the solution is placed on a glass slide for the CLSM measurement.

In Figure 1a, MF capsules with (PSS/PAH)$_5$ shell can be easily visualized by the circular red ring due to TRITC-dextran adsorption on the capsule wall. The emission from outside the capsule demonstrates there is TRITC-dextran in the solution. The red color is still appearing inside the capsule, indicating that the capsule allows the diffusion of TRITC-dextran of 66 kDa. It is a typical permeability behavior for the mesoporous capsules, who have mesh size greater than 18 nm.[8,35] To decrease the mesh size of capsules, the method of additional polyelectrolyte multilayers had been used to coat these porous capsules, as described in a previous paper.[36] Since the wall of the as-made mesoporous capsule remains charged to attract adsorption of oppositely charged polyelectrolytes, the additional polyelectrolyte multilayers are easily built up. After coating of one bilayer (or several bilayers up to four bilayers) of PSS/PAH, different permeability behaviors are established. Figure 1b shows that TRITC-dextran cannot penetrate into these PEM-coated capsules because no florescence intensity from TRITC is observed in the interior of the capsules. The mesh size of the capsule wall is greatly reduced by additional deposition of polyelectrolyte layer. Smaller sized dextran (4.4 kDa, radius 2.1 nm) is also prevented from diffusing through the PEM-modified capsule wall, indicating that the mesh size is roughly less than 4 nm (data not shown). Therefore, the original mesoporous capsules change to microporous ones after surface modification, inconsistent with the previous results.[36]

To show the influence of solvent treatment on the capsule permeability, the PEM-modified capsules are immersed in the mixed ethanol and water solvent with 60% ethanol for a longer time (more than 12 h). Then the permeability of dextran to capsules is characterized by CLSM. Figure 1d shows a red color in the interior region of capsules after 12 h after solvent treatment, which means TRITC-dextran is present in the interior of the capsules. The results confirm that the solvent-treated capsules allow the passing of both TRITC-dextran with 66 kDa (radius of 9 nm), where the original one does not. In addition, this solvent effect is time-dependent. In a short time (i.e., 1 h), only part of the capsules can allow the passing of probe material, as shown in Figure 1c. However, after 12 h, probes are permeable for all capsules, inconsistent with the in situ AFM results (see below). The results demonstrate that the mesh size or permeability of capsules can be tuned by solvent treatment. On the other hand, during the permeability measurement, we can neglect the slight changes of the hydrodynamic radius of dextran in the water−ethanol mixture. When the solvent-treated capsules are redispersed into the aqueous solution, their CLSM results with the same probes are similar to Figure 1c (data not shown), which indicates the increase of mesh size of capsules. In addition, the CLSM results also prove that the solvent treatment is an irreversible process, in agreement with the AFM and CV results (see below).

Upon the solvent treatment, the microporous capsules become mesoporous ones, which is described in the graphic

(Figure 1). Therefore, solvent effect can be utilized as a tool to control the diffusion of rigid and charge-free molecules such as dextran through the capsule wall by manipulating the mesh size of the capsules.

We also found that several circles of "PEM coating + solvent treatment" can alternately change the mesh size of capsules. However, the capsule will be eventually deformed because of the solvent-soften effect (the mechanical strength of the capsule is weakened).[28,31]

Solvent-Controlled Diffusion of PEM Films. As discussed before, PEM films on the mesoporous capsules show an important factor for controlling the mesh size of capsules. However, after solvent treatment, the PEM films on capsules lose the strength to prevent the diffusion of probes. Now attention is paid to the understanding of the mechanism of solvent-controlled permeability of PEMs. Electrochemical measurements are capable of detecting microstructural changes occurring inside the PEM film.[21,22,37−39] Cyclic voltammetry (CV) affords qualitative comparisons of permeation abilities among different films based on peak currents and voltammogram shape of the electrochemical probe molecule. The shape of the CV curves is capable of illustrating the molecular processes occurring at the electrode−film interface. $Fe(CN)_6^{3-/4-}$ is a well-studied redox probe and resembles one electron process in CV.[41] Thus, it is used as a probe to study the effect of solvent treatment on the permeability of the planar PEM film. Prior to the CV measurement, $(PSS/PAH)_n$ films are prepared on amine-terminated ITO. Here we use 10 bilayer PEMs ($n = 10$) to show the solvent effect on diffusion properties of probes because these film are continuous and defect-free and have a stronger response to solvent treatment.[42]

The diffusion of the electrochemical probe molecule, $Fe(CN)_6^{3-/4-}$, through the PEM film is strongly dependent on the film structure. For example, during the layer-by-layer assembly, different salt concentrations (0 M, 0.5 M, 1.0 M NaCl) are present in the polyelectrolyte solutions. Their CV profiles are different. The typical CV profiles of the PEM films prepared with 0.5 M NaCl are broad and plateau-shaped (Figure 2a, 0% ethanol), suggesting a current originating from an array of pinholes[41,43] or slow diffusion through the PEM films.[37] There is only a slight difference for peak currents and permeability of $(PSS/PAH)_{10}$ made in the presence of 0.5 and 1 M NaCl (Figure S2b in the Supporting Information), whereas the electrochemical behaviors of the PEM film made in the absence of salt (0 M NaCl) is evidently different. In the absence of salt, the redox probe shows a quasi-reversible CV; i.e., peak-to-peak separation is less than 100 mV (Figure S2c in the Supporting Information). This indicates that the probe diffuses freely through the layer and undergoes electron transfer reactions at the electrode. In contrast, the same PEM film prepared in the presence of salt (0.5M NaCl) is almost impermeable to the probe molecule (Figure 2a, 0% ethanol). The peak currents decrease by approximately 2 orders of magnitude, as shown in Figures 2b and 2c. The results demonstrate the sensitivity of CV measurements to the inner structure of the PEM films because it is known that the addition of salt screens the electrostatic interactions and leads to a dense and pore-free PEM film.[21,22,37−39]

To understand the effect of organic solvents on the PEM film structure, CV measurements are conducted in the mixed solvents of ethanol and water. Increase in the ethanol percentage has no apparent effect on the shape of CVs or peak currents when the PEM films are prepared from salt-free solutions as shown in Figure 2b. The CVs for $(PSS/PAH)_{10}$ films prepared from 0.5 and 1 M NaCl show the quasi-reversible voltammogram with a broad and plateau shape when the ethanol content is above 40% (Figure 2a and Figure S2b in Supporting Information). After 100 potential cycles, the shape and current of CVs are almost stable. A higher peak current is observed of PEM film treated with alcohol: for example, the peak current i_p of the $(PSS/PAH)_{10}$ film increases nearly 5-fold when immersed in 40% ethanol solution with respect to that in pure water (Figure 2c). The increase in i_p corresponds to increased permeability of the PEM toward redox ions. The increase in i_p at high ethanol concentration suggests some degree of polyelectrolyte complex rearrangement, which gives rise to chain aggregation and hole formation. We also found that such solvent effect is not dependent on the type of terminated layer. Similar results are observed with positive PAH as the outmost layer (Figure S3, Supporting Information), as compared with PSS-terminated film (Figure 2a).

Once the ethanol percentage is above 60%, a more complicated phenomenon is obtained (Figure S4, Supporting Information). The redox peaks split into two with potential cycles, signaling changes in the film structure. The i_p increases almost 10-fold. $Fe(CN)_6^{3-/4-}$ ions still maintain the same features except with smaller peak currents after rinsing with pure water or immersing them in salt solution (i.e., 0.05 M KCl). It is possible that immersion in 60% ethanol leads to large and permanent defects in the films and $Fe(CN)_6^{3-/4-}$ ions are still trapped within the film and cannot diffuse out. The permanent entrapment of ions may be due to the strong Coulomb interaction. The ion-exchange effect may be excluded since no release of ion in the film after a long immersion time in the salt solution. Although the phenomena are not completely understood until now, they provide important evidence of a local electrostatic effect due to the presence of organic solvents.

The stronger solvent effects are observed when films are treated with THF (Figure S5 in the Supporting Information). A similar trend is observed for the mixed solvents of THF and water except that changes in CVs occur at 40% THF.

Briefly, one can conclude that the addition of organic solvents enhances the permeability and entrapment of ions in PEM films. It shows that the solvent is another external stimulus, in addition to salt and pH,[37] that can be utilized for the control of transport and encapsulation capabilities of PEM films and capsules.

Solvent-Induced Morphology Changes of PEM Films. The enhanced permeability of polyelectrolyte multilayer either on a flat substrate or a porous template by solvent

---

(41) Chailapakul, O.; Crooks, R. M. *Langmuir* **1995**, *11*, 1329.
(42) Barreira, S. V. P.; Garcia-Morales, V.; Pereira, C. M.; Manzanares, J. A.; Silva, F. *J. Phys. Chem. B* **2004**, *108*, 17973.
(43) Menon, V. P.; Lei, J. T.; Martin, C. R. *Chem. Mater.* **1996**, *8*, 2382.

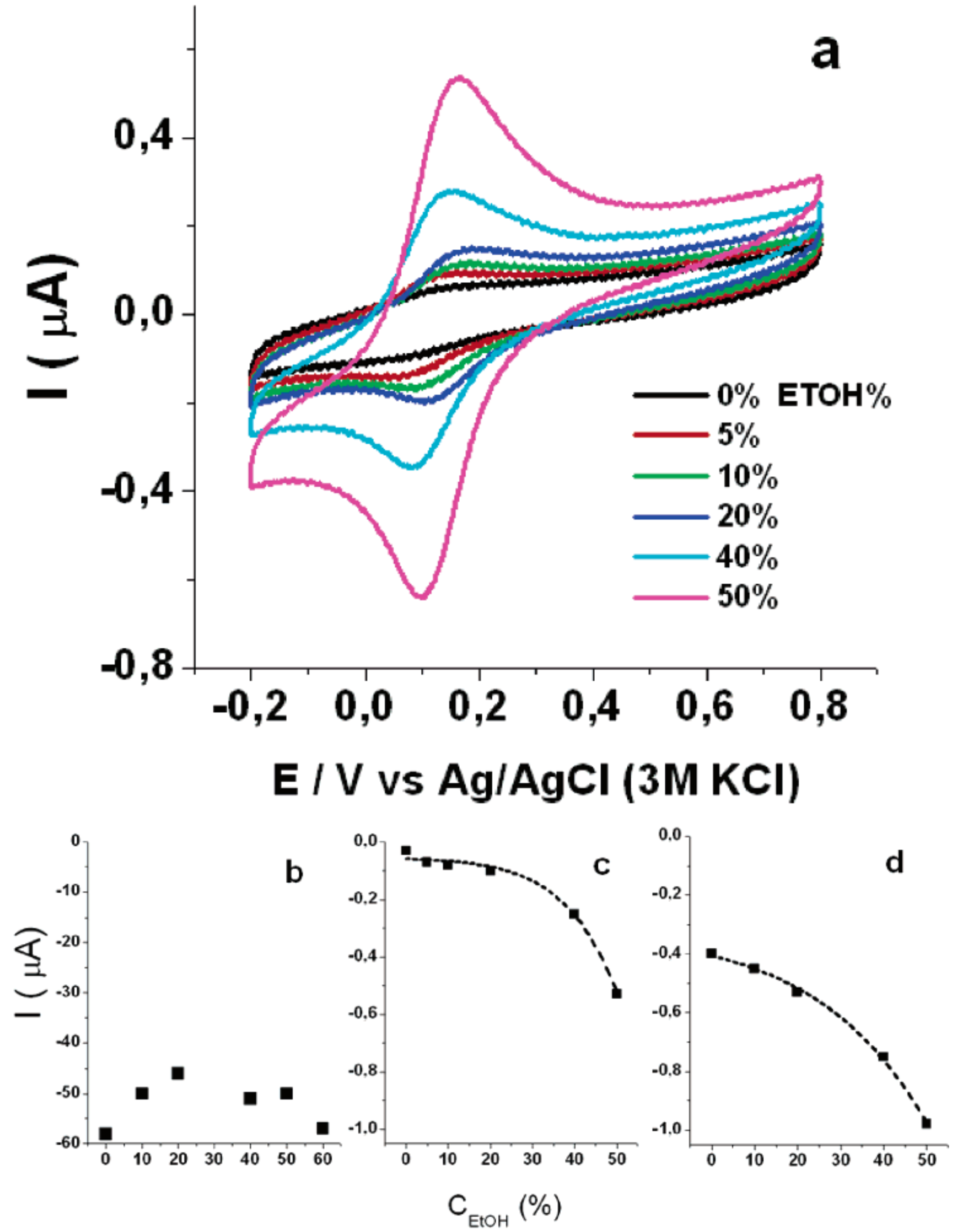

Figure 2. (a) Cyclic voltammograms of 5 mM $Fe(CN)_6^{3-/4-}$ at an ITO electrode coated with a $(PAH/PSS)_{10}$ film (made with 0.5 M NaCl). CVs were measured in water−ethanol solution, ethanol concentration: 0, 5, 10, 20, 40, and 50%. Cyclic voltammetry peak current values as a function of percentage of ethanol for PEM (b) made in the absence of salt; (c) made in 0.5 M NaCl, (d) made in 1.0 M NaCl, supporting electrolyte: 0.05 M KCl. (Scan rate 50 mV/s, average after three cycles).

treatment is demonstrated in last parts. The alteration of film permeability reflects the strong changes of microstructure within the polymeric thin films. Now the following question is how to find the evidence to show the changes of morphology and understand the mechanism of solvent effects. In this section, in situ AFM measurement is used to explore the phenomena.

Figure 3a shows a typical AFM image of the PEI/(PSS/PAH)$_2$ film obtained in deionized water. The film is devoid of large aggregates and has a surface roughness of $R_q = 0.57$ nm for a scan area of 0.5 × 0.5 μm^2. The same film imaged in 96% ethanol (Figure 3b) and 2-butanol (Figure 3c) shows aggregate and hole formation accompanied by a considerable increase in surface roughness. The holes in Figure 1b and 1c are quite uniform with an average diameter of 17 nm and depth of 2.5 nm, which is consistent with the CLSM results.

The film morphology is largely unchanged in the dry state after solvent removal as imaged in air (Figure 3d). Occasional large holes due to uneven evaporation are observed in the dried samples (Figure S6, Supporting Information). However, these big holes are not responsible for the solvent-controlled permeability behaviors.

The solvent-induced roughening of the PEM surface seems to be irreversible or at least exhibiting relaxation time longer than several hours because the film morphology does not revert back to the original state after reintroducing water into the AFM liquid cell.

AFM images have also been obtained in the mixed solvents of ethanol and water. Ethanol and water mixtures allow gradual changes of the solvent dielectric constant and polarity. When the ethanol volume percentage is less than 60%, no apparent morphological changes are observed on

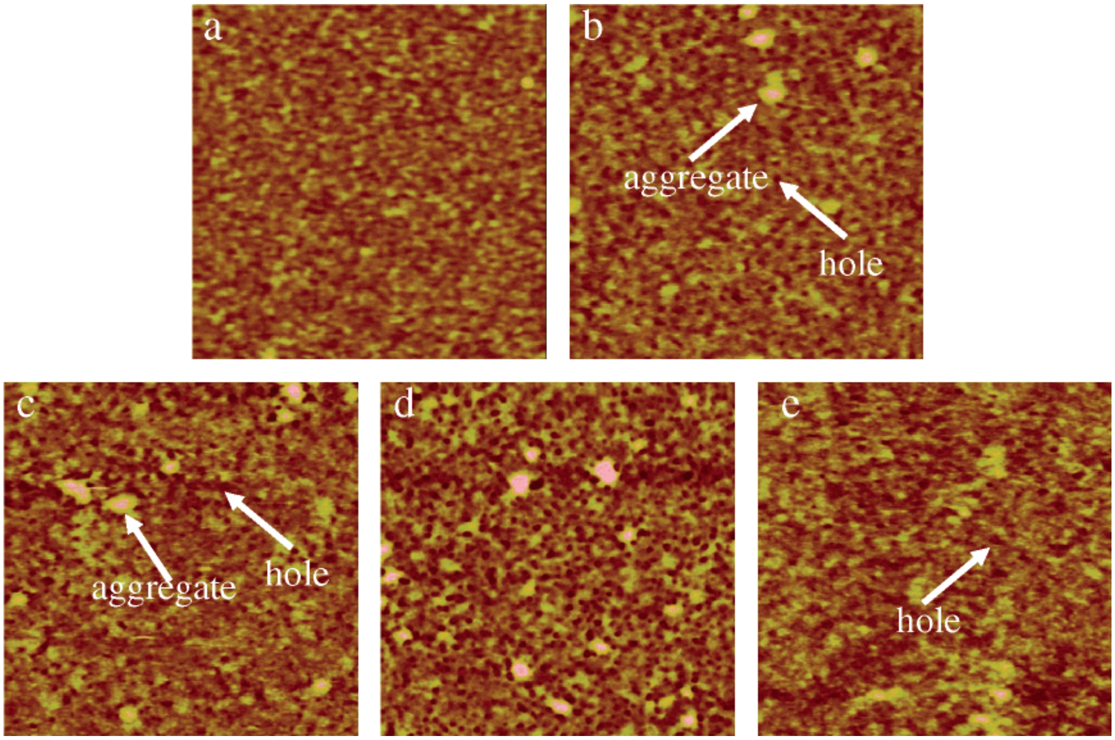

Figure 3. AFM height images with 1 × 1 μm^2 scan area and 10 nm z range of PEI−$(PSS/PAH)_2$ on mica captured in different solvents: (a) water (R_q = 0.57 nm); (b) 96% ethanol (R_q = 0.99 nm); (c) 2-butanol (R_q = 0.92 nm); (d) film of (c) imaged in air after 2-butanol evaporation (R_q = 0.95 nm); and (e) PEI/$(PSS/PAH)_4$ in 65% ethanol z range = 12 nm (R_q = 0.86 nm).

Scheme 1. Schematic Illustration of Solvent Influence on Microstructure of Polyelectrolyte Multilayers

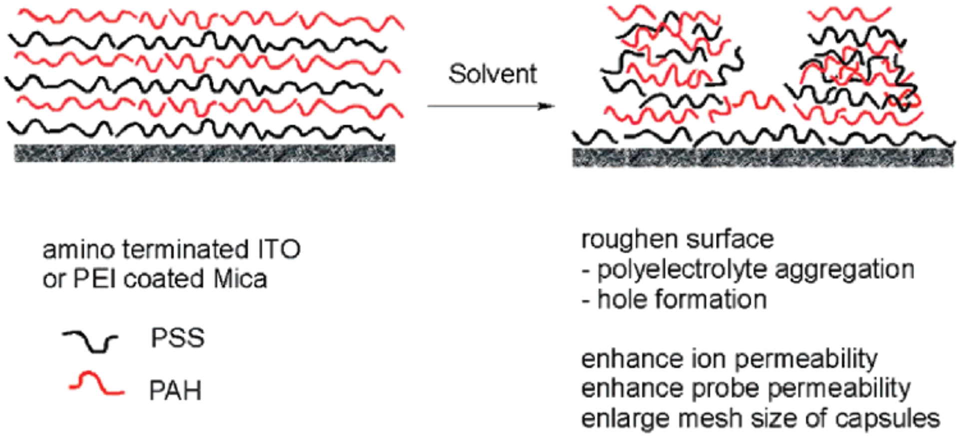

the PEM film surface by in situ AFM. The surface becomes rougher with holes developing above 60% ethanol. In this case, the dielectric constant of the solvent mixture is about 43. As compared to pure water (ϵ = 78.5), the Coulombic force increases by around 1.9 times in a 60% ethanol solvent mixture, based on eq 1 (see below). Figure 3e shows a typical AFM image of PEI/$(PSS/PAH)_4$ obtained in the mixed ethanol and water solvent with ethanol percentage greater than 60%. The surface roughness and the dimensions of the holes are similar to those in Figures 3b and 3c.

Our results suggest that the onset of solvent effect on film structure is around 60% ethanol by volume. However, the time dependence of film morphology changes still exists in the system. For the film with four bilayers of PSS/PAH, the mesopores can be clearly observed after 3 h (Figure S7, Supporting Information), which is consistent with CLSM experiments.

Reasonable Mechanism of Solvent Effect. With the addition of alcohol, pore-free and dense PEMs films have strong responses to the changes in local environment: The increase in surface roughness of PEM films and hole formation are observed. The fast diffusion of probe (small molecular weight ion) and the ion entrapment are demonstrated. The switched mesh size of capsules is beneficial for controlling the penetration of large macromolecules. These results cannot be concluded due to polyelectrolyte dissolution and removal from the PEM film. The main and possible reason is due to the decrease in solvent quality by increasing alcohol content.

It is known that increasing organic solvents content decreases the dielectric constants of mixture solution. The dielectric constants of water, ethanol, and 2-butanol are 78.5, 24.3, and 15.8, respectively. If using ethanol instead of water, the electrostatic attraction between polyelectrolyte segments will increase by almost a factor of 3, which is described by Coulombic force of

$$F = \frac{Q_1 Q_2}{4\pi\epsilon_0\epsilon r^2} \qquad (1)$$

Such strong attractive forces between the nearest opposite charge groups cause the polyelectrolyte complex to contract, to collapse, and to coagulate, as shown in Scheme 1. The rearrangement of the polyelectrolyte chains induce the formation of big aggregates and holes within the film, as revealed in the AFM images. In fact, the other interaction, for example, of dipole−dipole interaction, could also be involved in the microstructure changes due to the decreasing of the dielectric constant of the solvent. Therefore, the increased film inhomogeneity is responsible for the higher permeability of the PEM to redox ions as demonstrated by the CV measurements. The effects of solvent are summarized in Scheme 1. These findings show that the solvent is another controllable parameter for the tuning of film structure and permeability, which have potential applications in smart encapsulation and controlled delivery.

However, solvent effect is not a reversible process since the film morphology and permeability cannot revert back to the original ones for a long time. Several reasons point to this issue: First, it could be due to the long-term relaxation of polymer complex in the confined system. Second, it could be due to the strong electrostatic force between oppositely charged groups in the polyelectrolyte complex. For instance, during the polymer chain rearrangement process, unpaired charged groups have a priority in finding the other opposite ones to bind together quickly. After the solvent is changed back to a higher dielectric constant one, these new pairs cannot separate due to the strong interaction. In addition, the above-mentioned entrapment of $Fe(CN)_6^{3-/4-}$ in films seems to have a similar effect. Third, several other parameters could also be involved in these irreversible behaviors, such as temperature, moisture, and hydrogen bonding. (The degree of protonation of PAH will affect its H-bonding capacity with ethanol if the charge density of PAH should depend on the pH of the solutions.) To realize the reversible process by solvent treatment, more efforts must be directed toward seeking the other repulsive forces or interaction (i.e., covalent cross-links or pH response etc.) in order to balance the strong attractive Coulombic force.

Conclusions

In this paper, the effect of solvent on PEM film permeability and microstructure is investigated. Due to the strong Coulombic force in a low dielectric constant medium, the rearrangement of polyelectrolyte chains causes the increased surface roughness and aggregate/hole formation as compared with those in pure water, in agreement with AFM, CV, and CLSM results. AFM images obtained in 60 vol % or above ethanolic solutions and 2-butanol show the formation of nanometer-sized holes at the PEM film surface. The increased film heterogeneity also leads to increased permeation of probe material, $Fe(CN)_6^{3-/4-}$, through the PEMs as a result of ethanol addition. The probe material may be permanently trapped in the PEMs by forming ionic complexes with the polyelectrolytes, as it cannot be removed by water rinsing after the solvent treatment. On the other hand, solvent promotes the diffusion of large dextran molecules with molecular weight of 66 kDa through the otherwise impermeable shell of the PEM-modified capsules. The PEM-modified capsules are made by additional deposition of polyelectrolyte layers after core removal with mesh size reduction from more than 18 nm to less than 4 nm. The CLSM results show that the PEM-modified capsules can be easily penetrated by 66 kDa dextran (with hydrodynamic radius of 9 nm) after immersion of them in alcoholic solvents. These findings show that the solvent is another controllable parameter for the tuning of film structure and permeability, which have potential applications in smart encapsulation and controlled delivery.

Acknowledgment. The work has been supported by the Max-Planck-Society via a Fellowship to W. F. Dong. G. Mao acknowledges the National Science Foundation for financial support (CTS-0221586 and CTS-0216109).

Supporting Information Available: Additional figures including X-ray reflectivity patterns, cyclic voltammograms, and AFM height images. This material is available free of charge via the Internet at http://pubs.acs.org.

CM051090F